

RAIN DETECTING ACCURACY OF WEATHER RESEARCH FORECASTING (WRF) AND TRMM RAINFALL PRODUCT OVER CAMBODIA

Chhuonvuoch Koem, Sarintip Tantanee*

Department of Civil Engineering, Faculty of Engineering, Naresuan University, Phitsanulok 65000, Thailand

Article history

Received

21 August 2021

Received in revised form

25 November 2021

Accepted

01 December 2022

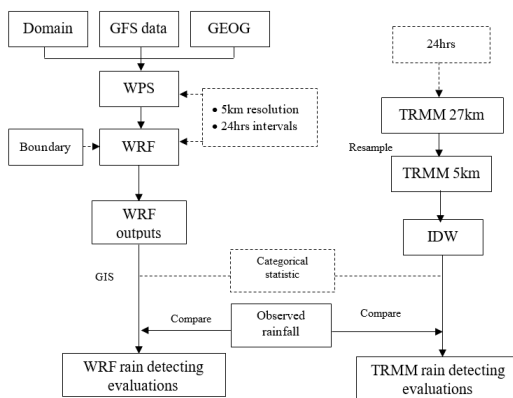
Published online

31 May 2022

*Corresponding author

sarintipt@nu.ac.th

Graphical abstract



Abstract

Rainfall is one of the important parameters for evaluating flood hazard risk. Cambodia is a vulnerable country to extreme rainfall where the number of rain gauges over the country is limited. Therefore, the possibilities of applying rainfall products from satellite observation and rainfall forecasting models are crucial for the country. The purpose of this research is to evaluate the detecting accuracy of the rainfall-based Weather Research Forecasting (WRF) model and TRMM rainfall products by comparing with observed rainfall during heavy rainfall for different topography over Cambodia. The categorical statistic is used to calibrate the rainfall from the WRF model with observed rainfall from 23 stations over Cambodia on selected heavy rainfall dates of 15, 17, and 19 September 2019. Cambodia experienced floods along the Tonle Sap River and the Mekong Basin by the triggered heavy rainfall. The results show that the detecting accuracy of days 15, 17, and 19 from TRMM rainfall matched with observed rainfall are 55%, 71%, and 63%, respectively. The average detecting accuracy of mountainous is 65% whereas plains are 63.33%. The average detecting accuracy of coastal and Tonle Sap is 53.66% and 63%, respectively. Moreover, the detecting accuracy of days 15, 17, and 19 forecasts from the WRF model compared with observed rainfall are 41%, 69%, and 63%, respectively. The average detecting accuracy of mountainous, plains, coastal, and Tonle Sap are 52%, 55.66%, 52.33%, and 65.66%, individually. The forecast rainfall from the WRF model and TRMM could detect the rainfall. They are therefore should be used in the areas that lack rainfall stations in Cambodia.

Keywords: WRF, TRMM, Rainfall, Categorical statistic, Cambodia

© 2022 Penerbit UTM Press. All rights reserved

1.0 INTRODUCTION

Rainfall is one of the most important hydrological components, which directly and indirectly affect the occurrence of disasters. The accuracy of rainfall measurement is significant to enhancing understanding of climate change [1], especially in Cambodia which is more vulnerable to extreme rainfall. The accurate rainfall is very valuable for the implication of flood [2] and drought hazard assessment [3], agricultural monitoring [4], and climate change analysis. The rainfall forecasting therefore must be accurate to obtain reliable data for effective monitoring and planning. Rain gauge is the most crucial way of

rainfall measurement, but the limitation of rain gauge density still exists due to the constraint of geological patterns and resources in several countries. Remote sensing has been shown greatly capable in rainfall estimation with the great spatiotemporal sampling density recently. The constraint however like clutter and blockage related to them reduce the data accuracy. In Cambodia, the rain gauges are very few (92 stations) and most of them were installed around the Tonle Sap Lake and the Mekong River [5] instead of in mountainous and steep areas. The average rain gauge data therefore may not well present the distribution of rainfall over the country. Therefore, several atmospheric models have been developed

to enhance and improve the understanding of weather forecasting.

Weather Research and Forecasting (WRF) is an advanced atmospheric model that can simulate both local and global forecasting. The WRF model is a mesoscale numerical weather model, which is widely used for weather prediction [6, 7] due to its advantages. The WRF model is considered for atmospheric research and operational estimating application that has two dynamical basics such as software architecture supporting system extensibility and parallel computation and data integration system. National Center for Atmospheric Research (NCAR), National Oceanic and Atmospheric Administration, U.S. Air Force, Naval Research Laboratory, University of Oklahoma, and Federal Aviation Administration (FAA) collaborated to progress WRF in the 1990s [8]. The WRF model has been applied in various atmospheric research in over 160 countries [9, 10]. Kaewmesri et al. [11] forecast a high-resolution WRF model for heavy rainfall in the southern part, of Thailand. Navale and Singh [12] used the WRF model to simulate the season-long rainfall over the North West Himalayan (NWH) region. Hodges and Klingaman [13] applied the WRF model to assess the tropical cyclone-related precipitation over the Northwest tropical pacific while Yik and Williams [14] used the model to identify the cold surge changing and their interface with the Madden Julian Oscillation (MJO) over Southeast Asia. Although simulated weather measurement may be carried out using several numerical approaches, those methods have their limitation. For the effectiveness of the model simulation, it required to assess the accuracy of the model is before it can be used in climate analysis since the bias can affect the efficiency of simulated results. The evaluation of simulated results from the WRF model is compared with observed rainfall from 23 stations over Cambodia. Observed rainfall is therefore used to validate the forecast rainfall from the WRF model over Cambodia by using categorical statistics. Moreover, satellite-based rainfall is determined to offer rainfall products at greater spatial and temporal resolution. Satellite-based rainfall from the Tropical Rainfall Measuring Mission (TRMM) however hindered by several problems such as spatiotemporal resolution differences. The satellite-based rainfall from TRMM has also been compared with observed rainfall to compare the accuracy between rainfall from WRF and TRMM. The purpose of this paper is to assess the rain detecting accuracy of 5 km resolution rainfall-based Weather Research Forecasting (WRF) and the accuracy of TRMM rainfall product by comparing with observed rainfall during the heavy rainfall on 15, 17, and 19 September 2019 overall regions in Cambodia.

2.0 METHODOLOGY

2.1 Study Area

Cambodia is located in the Southeast Asian region. It borders to the east with Vietnam, the West with Thailand, the north with Lao PDR, and the south with the Gulf of Thailand. It covers an area of 181,035 km². Cambodia is divided into four regions.

There are mountainous (Preah Vihear, Stung Treng, Kratie, Ratanak Kiri, Mondul Kiri, and Kampong Speu Provinces), plains (Takeo, Kandal, Prey Veng, Svay Rieng, Kampong Cham, Tboung

Khmum Province, and the Capital City of Phnom Penh), coastal (Koh Kong, Kampot, Kep, and Preah Sihanouk Provinces), and Tonle Sap (Pailin, Pursat, Kampong Thom, Siem Reap, Kampong Chhnang, Battam Bang, Banteay Meanchey, and Oddar Meanchey Provinces), as shown in Figure 1. The elevation ranges from 0 m to 1,814 m above the Mean Sea Level (MSL). Cambodia has two main seasons, the rainy and the dry season. The rainy season occurs from May to October while the dry season starts from November to April every year. The annual rainfall is 1,562 mm [2]. The average temperature is from 21 to 36 °C. The minimum temperature is in December and January whereas the maximum temperature is in April and May [15].

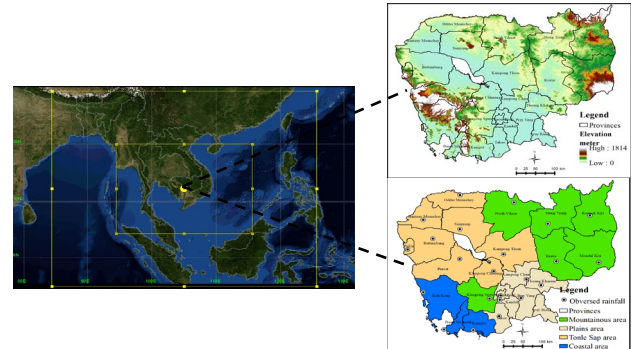


Figure 1 Study area covered Cambodia

2.2 METHOD

Figure 2 illustrates the conceptual framework of the research. Domain wizard was used to setting the research domain, which covers Cambodia. Global Forecast System (GFS) datasets were used to run the WRF model with the early conditions and lateral boundary settings to simulate three heavy rainfall events over Cambodia. The GFS datasets were taken from the Research Data Archive at the National Center for Atmospheric Research through the Website <https://rds.ucar.edu/datasets/>.

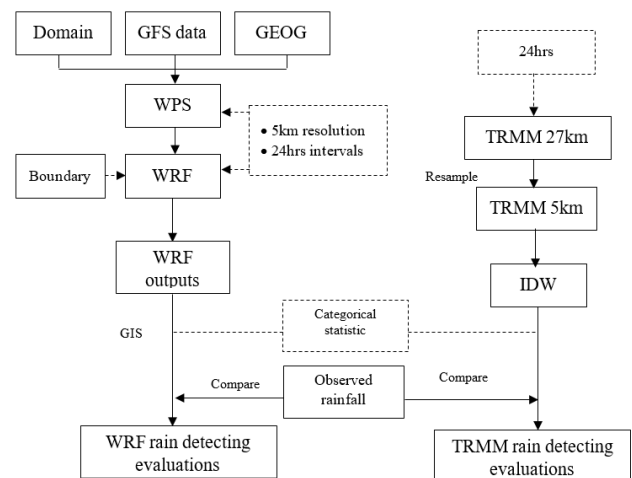


Figure 2 The conceptual framework of the study

Geographical static data (GEOG) were downloaded from the WRF User Page. Then all the data and information were used to run the WRF model at daily or 24 hours intervals with 5 km resolution. The WRF outputs, satellite-based rainfall from TRMM as well as country boundary were imported into GIS to

display the grid cell. Then the categorical statistic was applied to compare both rainfalls with observed rainfall. WRF, TRMM, and observed rainfall intensities were classified into three classes, which were little rain (0.01-10 mm), moderate rain (10-50 mm), and heavy rain (more than 50 mm).

The comparison of WRF and TRMM with observed rainfall has therefore based on the rainfall classification. Moreover, the comparison is also based on the regions of Cambodia namely, mountainous, plains, coastal, and Tonle Sap, as illustrated in Figure 1. The raster maps of WRF, TRMM, and observed rainfall were reclassified into three classes as mentioned earlier. The Extract Value to Points in Spatial Analysis Tool in GIS has been applied to obtain the value of each raster cell, which can be helpful for comparison processes.

2.2.1 Observed Rainfall

The observed rainfall from the Department of Meteorology, Ministry of Water Resource and Meteorology were applied to compare with the forecast rainfall of the WRF model in 3 days, 15, 17, and 19 September 2019. Due to the limitation of the rain gauge in Cambodia, 23 rainfall stations can be obtained, as shown in Figure 1. Table 1 illustrates the amount of rainfall on these three days along with the name and altitude of the station in Mean Sea Level (MSL). Inverse Distance Weight (IDW) interpolation tool in GIS has been applied to obtain the isohyet map, as presented in Figure 3.

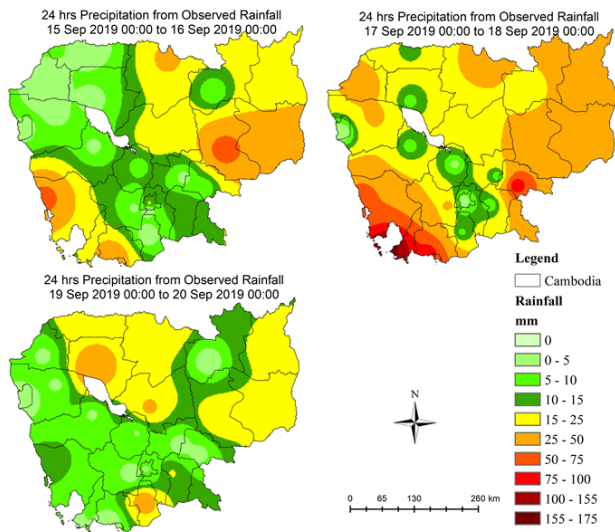


Figure 3 Isohyet map of rainfall on 15, 17, and 19 September 2019

Table 1 Observed rainfall on 15, 17, and 19 September 2019

Station	Lat.	Lon.	MSL	DAY 15	DAY 17	DAY 19
Battambang	13.1000	103.2000	13m	0.0	1.5	8.0
B. Meanchey	13.6167	102.9667	31m	0.0	1.5	9.0
K.Cham	12.0000	105.4500	14m	8.5	36.7	7.5
K.Chhnang	12.2167	104.6667	15m	0.0	3.9	51.5
Kohkong	11.6333	102.9833	13m	131.0	28.0	62.0
K.Speu	11.4667	104.5667	27m	14.5	8.0	0.0
K. Thom	12.6833	104.9000	13m	0.0	17.6	3.1
Kompot	10.6000	104.1833	4m	22.3	43.8	19.6
Kandal	11.4333	104.8167	8m	1.4	61.0	14.8
Kratie	12.4833	106.1667	23m	29.0	38.0	27.4
Mondolkiri	12.4500	107.1833	690m	53.2	71.8	2.0

Station	Lat.	Lon.	MSL	DAY 15	DAY 17	DAY 19
Prev Veng	11.4833	105.3167	13m	1.2	2.4	2.6
Pochentong	11.5500	104.8333	11m	21.2	8.6	0.0
Pailin	12.8000	102.6000	170m	60.0	2.0	30.0
Preh Vihear	14.1000	105.1500	62m	0.0	2.0	17.4
Pursat	12.5500	103.8500	18m	43.8	0.8	0.8
Ratanakiri	13.7333	106.9833	330m	3.5	30.0	49.5
Stung Treng	13.5167	105.9667	54m	0.0	2.0	24.4
Svay Rieng	11.8333	105.8000	6m	0.0	24.0	0.0
Siem Reap	13.3667	103.8500	15m	8.2	2.4	47.8
Sihanoukville	10.6167	103.4833	13m	36.8	100.8	1.4
Takeo	10.9833	104.8000	6m	0.0	14.0	0.0
O. Meanchey	14.3000	103.8500	-	2.1	8.5	2.1

2.2.2 Trmm 3b42v7

The rainfall data of TRMM 3B42V7 in gridded format with 24 hours temporal resolution were applied in this research. The spatial resolution is 0.25° or approximately 27 km. The TRMM data estimations are created by adjusted microwave precipitation estimations that are additional joint with infrared estimates. The TRMM data were downloaded on days 15, 17, and 19 September 2019, which is consistent with the simulated rainfall from the WRF model. The downloaded data, therefore, was resampled to 5 km to compare the spatial resolution of simulated rainfall by using the Bilinear resampling method, which uses the weighted average values of the four nearest cells to define the value on the output raster. Figure 3 shows the daily rainfall on 15, 17, and 19 September 2019 over Cambodia from TRMM after resampling with a spatial resolution of 5 km.

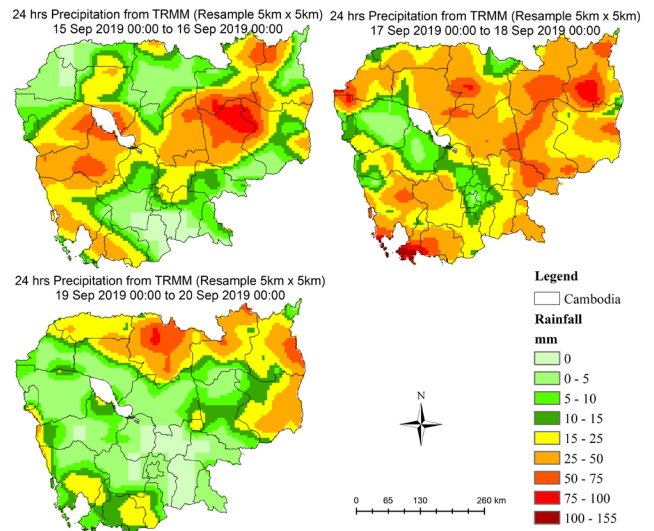


Figure 4 Satellite-based rainfall from TRMM on 15, 17, and 19 September 2019

2.2.3 Wrf Forecasting

Weather Research Forecasting (WRF) model is a greatly convenient, effective, and broadly used tool to bring out atmospheric simulations. Daily simulation (24 hours interval) on 15, 17, and 19 September 2019 was carried out with highlighting the heavy rainfall day over Cambodia. The WRF model was applied to forecast the rainfall during these three days. There are several steps to compile the WRF model such

as system environment tests, building libraries, library compatibility tests, building WRF, building WPS, static geography data, real-time data, and running WPS and WRF. The WRF model was run on Linux by using the MobaXterm program. Global Forecast System (GFS) data were downloaded from the National Weather Service (NCEP) at no charge. The data are generated by using the Global Forecast System (GFS) Model. NCEP provides the GFS data every day. Likewise, geographical static was also used, and it was downloaded from the WRF Users Page. A nested domain wizard was applied to set the study domain in WRF configuration to acquire the rainfall at a better resolution and lessen the computing measure. The experiment domain extent is from 94° E to 116° E and from 4° N to 20° N, as shown in Figure 5. Simulated rainfall datasets consistent with the nested domain with 5 km resolution were assessed against the observed rainfall for the evaluation of the WRF model in simulating high-resolution heavy rainfall over Cambodia.

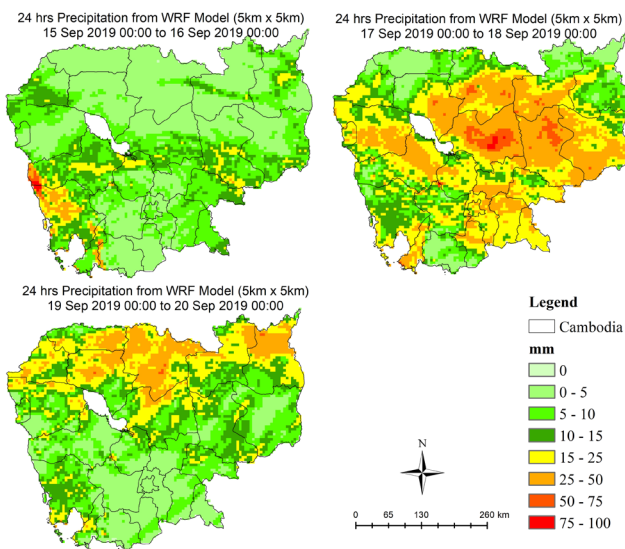


Figure 5 Accumulated rainfall from WRF model on 15, 17, and 19 September 2019

2.2.4 COMPARISON TECHNIQUES

Since the rainfall data are observed and simulated as discrete values, the categorical statistics were applied to define how good the simulated rainfall from the WRF model is. The categorical statistics were used in several studies for validation, comparison, and verification of satellite data and WRF outputs [1, 7, 12, 16]. The scores were calculated to compare the observed rainfall with satellite-based rainfall TRMM and observed rainfall with WRF outputs in taking the amount of rainfall over Cambodia. Table 2 illustrates a 3 x 3 contingency table that has been created for the three potential outcomes. Then the scores were considered due to the values of the hit, miss, and false alarm. Hit is the number of predicted times for each criterion that the expected event occurs. False alarm means the number of times the simulated rainfall occurs, but observed rainfall does not occur. Miss refers to the number of times simulated rainfall does not occur, but the observed rainfall occurs.

Table 2 Contingency table for comparing WRF and TRMM with observed rainfall

	Little rain	Moderate rain	Heavy rain
Little rain	hit	miss	miss
Moderate rain	false alarm	hit	miss
Heavy rain	false alarm	false alarm	hit

It is significant to apply different metrics to test the errors since a single error metric divulges only inadequate information about an error.

- False alarm ratio (FAR): the falsely detected rain pixels divided by the entire rain pixels as simulated by the WRF model (Eq. 1). Near or equal to zero is the best result.

$$FAR = \text{false alarm} / (\text{hits} + \text{false alarm}) \quad (1)$$

- Frequency bias index (FBI): the ratio of simulated rainfall events to the satellite-based rainfall events measures if the simulated rainfall is overestimating or underestimating the frequency of rainfall events (Eq. 2). The best score is 1 while minor or greater than 1 defines underestimation or overestimation of the occurrence of rainfall events, individually.

$$FBI = (\text{hit} + \text{false alarm}) / (\text{hit} + \text{miss}) \quad (2)$$

- Probability of detection (POD): the rainfall measures that were correctly simulated by the WRF model. POD can be calculated by using Eq. 3. Its value is between 0 and 1, and 1 is the best result.

$$POD = \text{hit} / (\text{hit} + \text{miss}) \quad (3)$$

- Accuracy: the agreement of the WRF model and TRMM on detection of the rainfall occurrences can be calculated by using Eq. 4. The desired score is 1.

$$\text{Accuracy} = (\text{hit} + \text{correct with no rain}) / \text{total} \quad (4)$$

3.0 RESULTS AND DISCUSSION

3.1 Trmm And Observed Rainfall

The satellite-based rainfall from TRMM was compared with the observed rainfall over Cambodia and each region by using the categorical statistic to find the values of False Alarm Ratio (FAR), Frequency Bias Index (FBI), Probability of Detection (POD), and Accuracy of TRMM data, as shown in Table 3. The overall False Alarm Ratio (FAR) in these three days ranges between 0.17 and 0.29. Besides, the FAR value on day 19 is 0.17, which is the desired result (near zero), and it is followed by day 17 (0.21) and day 15 (0.29). The FAR values on both days 17 and 19 in plains (0.11 and 0.02, respectively) and Tonle Sap (0.11 and 0.09, respectively) regions explain good results compared to other regions. The Frequency Bias Index (FBI) in the comparison of TRMM and observed rainfall is acceptable. The overall result of FBI on day 15 is the greatest with a value of 1.00 whereas on day 19 is 0.88. The FBI value on day 17, however, is greater than one (1.12), which means that the satellite-based rainfall from TRMM overestimates the observed rainfall. Furthermore, the overestimated rainfall from satellite-based is found in Tonle Sap region on day 15, and the mountainous and coastal region on both days 17 and 19. The Probability of Detection (POD) overall value on 15, 17, and 19 is very significant with the value of 0.71, 0.88, and 0.73, respectively. It specifies that satellite-based rainfall from

TRMM can fairly detect the hits (rainfall) over Cambodia. The accuracy of satellite-based rainfall from TRMM over Cambodia is quite good with the percentage of 55%, 71%, and 63% on 15, 17, and 19, respectively. These results indicate that the satellite-based rainfall can be represented the observed rainfall but with limited accuracy. On day 15, the accuracy in the mountainous region is fairly low (0.46) compare to other regions whereas accuracy on both days 17 and 19 is low in the coastal region (0.41 and 0.39, respectively). The accuracy of other regions, however, is very satisfactory.

Table 3 Error metrics of TRMM and observed rainfall

		Mountainous	Plains	Coastal	Tonle Sap	Cambodia
DAY 15	FAR	0.28	0.19	0.01	0.41	0.29
	FBI	0.78	0.75	0.82	1.54	1.00
	POD	0.57	0.61	0.82	0.91	0.71
	Accuracy	0.46	0.53	0.81	0.56	0.55
DAY 17	FAR	0.22	0.11	0.59	0.11	0.21
	FBI	1.25	0.99	2.41	0.88	1.12
	POD	0.98	0.88	0.98	0.78	0.88
	Accuracy	0.77	0.79	0.41	0.71	0.71
DAY 19	FAR	0.17	0.02	0.55	0.09	0.17
	FBI	1.02	0.60	1.67	0.72	0.88
	POD	0.85	0.59	0.75	0.66	0.73
	Accuracy	0.72	0.58	0.39	0.62	0.63

The accuracy of satellite-based rainfall from TRMM compared with observed rainfall from 23 stations over Cambodia on day 15 is not very good even though the results on days 17 and 19 are better. The number of missed rainfall in the comparison results of day 15 is quite higher than the other days with a total value of miss 3,953 whereas on days 17 and 19 are 1,597 and 1,771, respectively. The total value is 7,290. Tian, Peters-Lidard [17] also presented in their study that 3B42V7 still has higher missed rainfall events when calibrated with rainfall stations. On the other hand, non-rainfall cirrus clouds up in high altitudes up to 18 km can simply be a mistake as rainy clouds by the satellite foremost to following false alarms and overestimation of rainfall [1]. TRMM however still be convenient in the mountainous regions where the rainfall stations are limited.

3.2 Wrf And Observed Rainfall

Table 4 presents the error metrics of categorical statistics of forecast rainfall from the WRF model compared with observed rainfall from 23 stations over Cambodia. The error metrics calculated for different ranges are also divided into four regions such as mountainous, plains, coastal, and Tonle Sap regions. The False Alarm Ratio (FAR) values during days 15, 17, and 19 are 0.10, 0.11, and 0.17, respectively, over the study areas. In mountainous, plains, and coastal regions on day 15 and mountainous areas on day 17, the FAR values (0.02, 0.03, 0.03, and 0.03, respectively) are the lowest compared to other regions of each day. The Frequency Bias Index (FBI) values on days 15, 17, and 19 were found to be changing from 0.48 to 0.87 with the lowest value observed on day 15. FBI value on

day 17 is 0.86. Moreover, the FBI value in the plains region explains a very good result with a value of 0.96 then followed by the Tonle Sap region on the same day and the Tonle Sap region on day 15 with the value of 0.85 and 0.82, respectively. However, the FBI value in the coastal region on day 17 and coastal and Tonle Sap regions on day 19 seems to be greater than other regions with the value of 1.10, 1.13, and 1.06. It, therefore, indicates that the WRF model overestimates the frequency of rainfall from observed stations. The higher Probability of Detection (POD) values specifies the WRF model's capability to identify the hits. It can be seen that the POD value on day 17 is the greatest result, and it is followed by day 19 and day 15 with the value of 0.76, 0.72, and 0.43, respectively. Plains region on day 17 has the highest values of POD with the value of 0.85 as well as Tonle Sap region on day 19. Likewise, the POD values on day 17 are very good compared to other days. On day 19, the overall POD value is also very good (0.72); however, POD values in the plains region seem to be average (0.46). This indicates that the WRF model predicted the rainfall in these two days seems to be more agree with the observed rainfall. The maximum accuracy percentage is 69% (0.69) on day 17 whereas the accuracy of the WRF model compared with observed rainfall on day 19 and day 15 are 63% (0.63) and 41% (0.41), respectively. The accuracy of the WRF model in mountainous and plains regions on day 17 however seems to be good with values of 0.73 and 0.76, respectively. It can identify that the WRF model also gives desired values compared with observed rainfall.

Table 4 Error metrics of WRF and observed rainfall

		Mountainous	Plains	Coastal	Tonle Sap	Cambodia
DAY 15	FAR	0.02	0.03	0.03	0.16	0.10
	FBI	0.19	0.49	0.52	0.82	0.48
	POD	0.18	0.48	0.50	0.69	0.43
	Accuracy	0.18	0.47	0.49	0.61	0.41
DAY 17	FAR	0.03	0.11	0.31	0.14	0.11
	FBI	0.78	0.96	1.10	0.85	0.86
	POD	0.75	0.85	0.75	0.74	0.76
	Accuracy	0.73	0.76	0.56	0.66	0.69
DAY 19	FAR	0.11	0.11	0.35	0.20	0.17
	FBI	0.79	0.52	1.13	1.06	0.87
	POD	0.70	0.46	0.73	0.85	0.72
	Accuracy	0.65	0.44	0.52	0.70	0.63

The results were acquired through a selection of statistical evaluations following the regions. The main purpose of conducting this research over different regions was to detect WRF behavior in different places compared with observed rainfall. The amount of rainfall underestimate is greater than the overestimated rainfall over all regions in Cambodia. The average result of the FAR value is 0.13 (zero is the perfect value). The average FBI, POD, and Accuracy values are 0.74, 0.64, and 0.58, respectively, while one is the desired value. The WRF model compared with observed rainfall shows average results. Additionally, the results of the comparison of forecast rainfall from WRF and observed rainfall illustrate that the FAR value on day 15 is better than on days 17 and 19 whereas FBI, POD, and Accuracy values on both days 17 and 19 are greater

than the forecast than day 15 in all regions. It could be related to the rainfall occurrence on that day. There was rainfall everywhere on day 17 whereas, on day 19, rainfall occurred in almost all the stations except Kampong Speu, Pochentong, and Svay Rieng Stations. There were however eight stations, Battambang, Banteay Meanchey, Kampong Cham, Kampong Thom, Preh Vihear, Stung Treng, Svay Rieng, and Takeo Stations, did not receive any rainfall on day 15 (Table 1). Likewise, the uncertainties may arise from how observed rainfall data were used or deficient spatial representation of observed rainfall to obtain the raster grid cells [18]. It also could be due to the limitation of observed rainfall over Cambodia due to many of the existing rainfall station records are not completed. The results also show that the WRF model is highly sensitive to the orographic regions, and it can resolve the problem of mountainous rainfall with the steepness region well [7]. Figure 6 presents the FAR, FBI, POD, and Accuracy values of WRF and TRMM compared with observed rainfall on days 15, 17, and 19 in all regions over Cambodia.

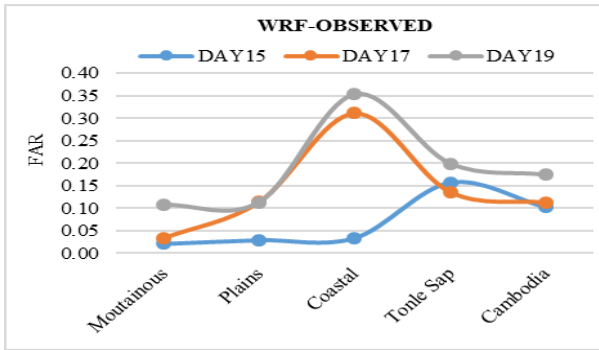


Figure 6 False Alarm Ratio (FAR) of WRF

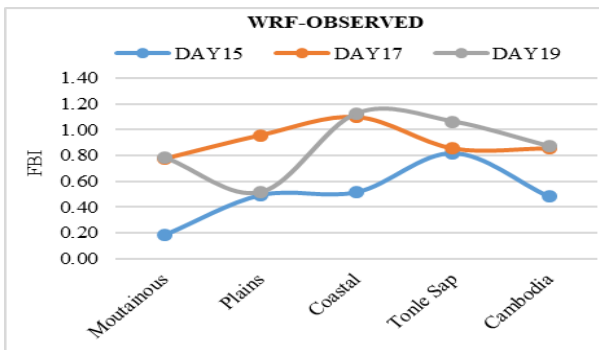


Figure 7 Frequency Bias Index (FBI) of WRF

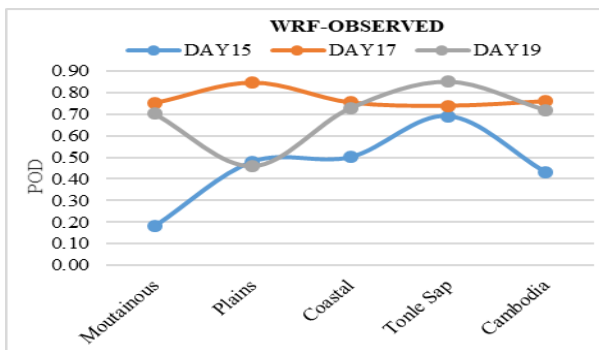


Figure 8 Probability of Detection (POD) of WRF

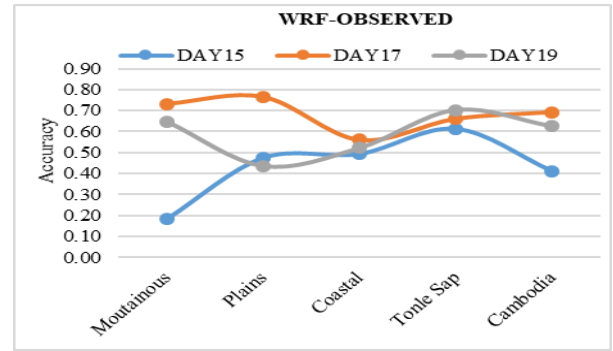


Figure 9 Accuracy of WRF

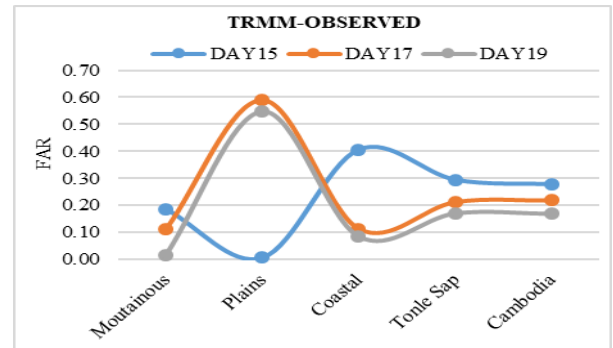


Figure 10 False Alarm Ratio (FAR) of TRMM

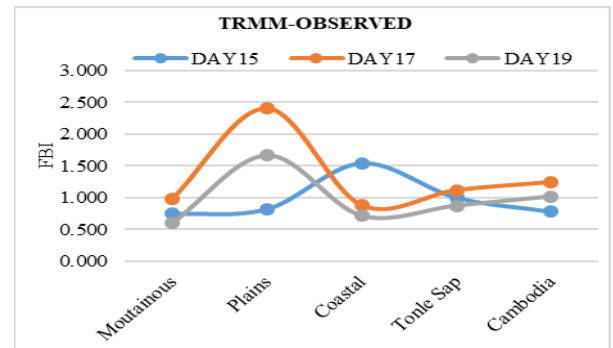


Figure 11 Frequency Bias Index (FBI) of TRMM

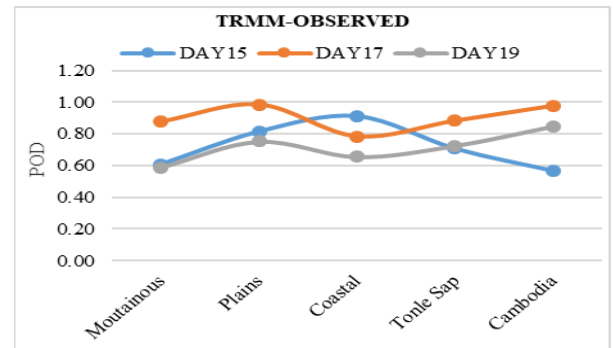


Figure 12 Probability of Detection (POD) of TRMM

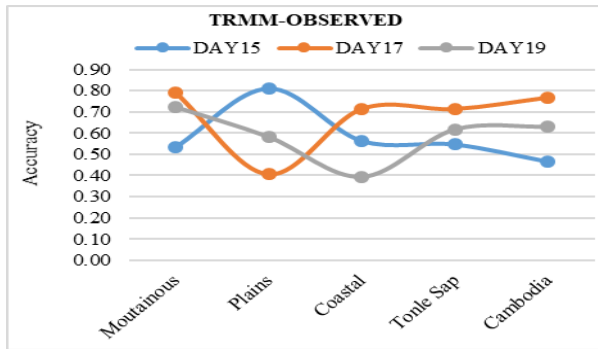


Figure 13 Accuracy of TRMM

The finding is very beneficial for an enhanced sympathetic of the spatial pattern of rainfall over all the regions of Cambodia. The observed rainfall stations are too few in the mountainous region whereas satellite-based rainfall reclamation affects mountainous terrain, which causes high bias. It is, therefore, crucial to have data from many observed rainfall stations to improve the comprehensive assessment of WRF model simulation in all regions of Cambodia. The comparison of forecast rainfall from the WRF model and satellite-based rainfall from TRMM with observed rainfall illustrates that the average values of FBI, POD, and Accuracy of TRMM are quite well than the WRF model even though the average FAR value of the WRF model is better. It means that satellite-based rainfall from TRMM is greater than the WRF model in the comparison with 23 rainfall stations over Cambodia on days 15, 17, and 19 of September 2019. The accuracy of satellite-based rainfall over the mountainous region from TRMM is better than WRFs in all three days compared. It's therefore significant to use satellite-based rainfall from TRMM since it hardly has the stations. The resolution of satellite-based rainfall from TRMM is approximately 27 km which might cause some bias in the reporting data while the resolution of the WRF model can be adjusted.

4.0 CONCLUSION

A detailed comparison of forecast rainfall from the WRF model and satellite-based rainfall from TRMM with 23 stations of observed rainfall provides a chance to understand the level of uncertainties in the data creation and tile the way for more development. The observed rainfall stations over Cambodia are still uncovered in many regions, so they can be subjected to various errors in measurement and comparison approaches. Satellite-based rainfall from TRMM is gauge-corrected data that could be represented the observed rainfall in a limited condition because of its bias level. The current study used categorical metrics to assess the potential of the WRF model and TRMM to detect rainfall over all regions in Cambodia. This study only focused on the rainfall occurrence, the extract amount of rainfall was not discussed. Further study therefore should be done to detect the amount of rainfall. Moreover, the study put more attention on WRF's performance in each region to obtain the information on rainfall bias as a meaning of regions even the performance of the WRF model can be assessed over different spatiotemporal scales. The overall detected rainfall from satellite-based TRMM is quite better

than the WRF model even though the detected rainfall from WRF over the coastal region on days 17 and 19 is more satisfactory than TRMM. A better-observed rainfall is required for overall regions in Cambodia to evaluate the WRF model more precisely.

Acknowledgment

The authors would like to acknowledge the Ministry of Water Research and Meteorology, especially the Department of Meteorology, for supporting data for studying and analyzing the accuracy of the rainfall forecast for Cambodia.

References

- [1] Bhart, V., & Singh, C. 2015. Evaluation of error in TRMM 3B42V7 precipitation estimates over the Himalayan region. *Journal of Geophysical Research: Atmospheres*, 120(24):12458-12473. DOI: <https://doi.org/10.1002/2015JD023779>
- [2] Koem, C., & Tantane, S. 2020. Flash flood hazard mapping based on AHP with GIS and satellite information in Kampong Speu Province, Cambodia. *International Journal of Disaster Resilience in the Built Environment*, 12(5): 457-470. DOI: <https://doi.org/10.1108/IJDRBE-09-2020-0099>
- [3] Palchoudhuri, M., & Biswas, S. 2016. Application of AHP with GIS in drought risk assessment for Puruliya district, India. *Natural Hazards*, 84(3): 1905-1920. DOI: <https://doi.org/10.1007/s11069-016-2526-3>
- [4] Chhinh, N., & Millington, A. (2015). Drought Monitoring for Rice Production in Cambodia. *Climate*, 3(4), 792-811.
- [5] Koem, C., & Tantane, S. (2021). Flood Disaster Studies: A Review Of Remote Sensing Perspective In Cambodia. *Geographic Technica*, 16(1): 13-24. DOI: https://doi.org/10.21163/GT_2021.161.02
- [6] Srinivas, C. V., Yesubabu, V., Hari Prasad, D., Hari Prasad, K. B. R. R., Greeshma, M. M., Baskaran, R., & Venkatraman, B. 2018. Simulation of an extreme heavy rainfall event over Chennai, India using WRF: Sensitivity to grid resolution and boundary layer physics. *Atmospheric Research*, 210: 66-82. DOI: <https://doi.org/10.1016/j.atmosres.2018.04.014>
- [7] Navale, A., & Singh, C. 2020. Topographic sensitivity of WRF-simulated rainfall patterns over the North West Himalayan region. *Atmospheric Research*, 242, 105003. DOI: <https://doi.org/10.1016/j.atmosres.2020.105003>
- [8] Sorooshian, S., Hsu, K., Gao, X., Li, J., AghaKouchak, A., & Nasrollahi, N. 2012. Assessing the Impacts of Different WRF Precipitation Physics in Hurricane Simulations. *Weather and Forecasting*, 27(4): 1003-1016. DOI: <https://doi.org/10.1175/WAF-D-10-05000.1>
- [9] El Afandi, G., Morsy, M., & El Hussieny, F. 2013. Heavy Rainfall Simulation over Sinai Peninsula Using the Weather Research and Forecasting Model. *International Journal of Atmospheric Sciences*, 2013: 1-11. DOI: <https://doi.org/10.1155/2013/241050>
- [10] Kaewmesri, P., Humphries, U., Wangwongchai, A., Wongwies, P., Archevarapuprok, B., & Sooktawee, S. 2017. The Simulation of Heavy Rainfall Events over Thailand Using Microphysics Schemes in Weather Research and Forecasting (WRF) Model. *World Applied Sciences*, 35(2): 310-315. DOI: 10.5829/idosi.wasj.2017.310.315
- [11] Kaewmesri, & et al. 2017. Simulation on high-resolution WRF model for an extreme rainfall event over the southern part of Thailand. *International Journal of Advanced And Applied Sciences*, 4(9): 26-34. DOI: <https://doi.org/10.21833/ijaas.2017.09.004>
- [12] Navale, A., Singh, C., Budakoti, S., & Singh, S. K. 2020. Evaluation of season long rainfall simulated by WRF over the NWH region: KF vs. MSKF. *Atmospheric Research*, 232: 104682. DOI: <https://doi.org/10.1016/j.atmosres.2019.104682>
- [13] Hodges, K. I., Klingaman, N. P., & Peatman, S. C. 2019. Tropical Cyclone-Related Precipitation over the Northwest Tropical Pacific in Met Office Global Operational Forecasts. *Weather and Forecasting*, 34(4): 923-941. DOI: <https://doi.org/10.1175/WAF-D-19-0017.1>
- [14] Yik, D. J., Williams, K. D., Tangang, F., Permana, D., Marzin, C., Handayani, A. S., Xavier, P. 2020. Seasonal Dependence of Cold Surges and their Interaction with the Madden-Julian Oscillation over

- Southeast Asia. *Journal of Climate*, 33(6): 2467-2482. DOI: <https://doi.org/10.1175/JCLI-D-19-0048.1>
- [15] CFE-DM. 2017. *Cambodia Disaster Management Handbook*. Phnom Penh, Cambodia: Center for Excellence in Disaster Management & Humanitarian Assistance.
- [16] Yi, L., Zhang, W., & Wang, K. 2018. Evaluation of Heavy Precipitation Simulated by the WRF Model Using 4D-Var Data Assimilation with TRMM 3B42 and GPM IMERG over the Huaihe River Basin, China. *Remote Sensing*, 10(4): 646. DOI: <https://doi.org/10.3390/rs10040646>
- [17] Tian, Y., Peters-Lidard, C. D., Eylander, J. B., Joyce, R. J., Huffman, G. J., Adler, R. F., Zeng, J. 2009. Component analysis of errors in satellite-based precipitation estimates. *Journal of Geophysical Research*, 114(D24). DOI: <https://doi.org/10.1029/2009JD011949>
- [18] Su, F., Hong, Y., & Lettenmaier, D. P. 2008. Evaluation of TRMM Multisatellite Precipitation Analysis (TMPA) and Its Utility in Hydrologic Prediction in the La Plata Basin. *Journal of Hydrometeorology*, 9(4): 622-640. DOI: <https://doi.org/10.1175/2007JHM944.1>